processes

MDPI

Article

The Effect of Mineralized Plasmatic Matrix and Chitosan on the Healing of Critical-Sized Mandibular Bone Defects in a Rabbit Model

Ahmed Hendawy [1], Ayman Atiba [1], Walied Abdo [2], Amira Osman [3], Abdelfattah Sadakah [4], Ashraf Abou ElReash [5], Gamal Elsayad [1] and Xiaoli Xie [6,*]

1 Department of Surgery, Anesthesiology, and Radiology, Faculty of Veterinary Medicine, Kafrelsheikh University, Kafrelsheikh 33516, Egypt
2 Department of Pathology, Faculty of Veterinary Medicine, Kafrelsheikh University, Kafrelsheikh 33516, Egypt
3 Department of Histology, Faculty of Medicine, Kafrelsheikh University, Kafrelsheikh 33516, Egypt
4 Department of Maxillofacial Surgery, Faculty of Dentistry, Tanta University, Tanta 31527, Egypt
5 Conservative Department, Faculty of Dentistry, Delta University for Science and Technology, Jamasah, Ad Daqahliyah 7730103, Egypt
6 Hunan Clinical Research Center of Oral Major Diseases and Oral Health & Xiangya Stomatological Hospital & Xiangya School of Stomatology, Central South University, Changsha 410008, China
* Correspondence: xiexiaoli@csu.edu.cn

Abstract: Background: In maxillofacial surgery, critical size mandibular defects remain a challenging issue. There have been numerous attempts to improve mandibular defect healing. Recently, bone tissue engineering has provided many benefits in improving bone healing. Herein, we tried to investigate the effect of Mineralized plasmatic matrix (MPM) and Chitosan to enhance tissue healing and regeneration in mandibular bone defect. Methods: A mandibular bone defect of critical size was created in 45 New Zealand rabbits. There were three groups of rabbits: the MPM group, the Chitosan group, and the control group. Radiographical, histological, and immune histochemical evaluations were performed at 4, 8, and 12 post-operative weeks. Results: The MPM group demonstrated the highest degree of bone formation with uniform radio-opacity nearly like that of adjacent healthy parent tissue. While in the chitosan group, most of the defect area was filled with radio-opaque bone with persistent small radiolucent areas. The control group showed less bone formation than the MPM and chitosan group, with more radiolucent areas. Sections stained with (H&E) demonstrated an increase in osseous tissue formation in both the MPM and chitosan groups. Staining with Masson's trichrome revealed an increase in fibrous connective tissue proliferation in both the MPM and chitosan groups. In both the MPM and chitosan groups, nuclear factor kappa p65 was downregulated, and matrix metalloproteinase-9 was upregulated. Conclusion: According to the current study, MPM and Chitosan may have beneficial effects on the healing of critical-sized mandibular bone defects.

Keywords: mineralized plasmatic matrix; chitosan; mandibular bone defect; MMP9; NF-κB; rabbit

Citation: Hendawy, A.; Atiba, A.; Abdo, W.; Osman, A.; Sadakah, A.; Abou ElReash, A.; Elsayad, G.; Xie, X. The Effect of Mineralized Plasmatic Matrix and Chitosan on the Healing of Critical-Sized Mandibular Bone Defects in a Rabbit Model. *Processes* **2022**, *10*, 1890. https://doi.org/10.3390/pr10091890

Academic Editor: Maurizio Ventre

Received: 15 August 2022
Accepted: 13 September 2022
Published: 18 September 2022

1. Introduction

Bone healing is a sequence of intricately orchestrated biological events. It includes osteoinduction and osteoconduction via intracellular and extracellular signaling pathways in diverse cell types [1]. Critical bone defects can be caused by congenital defects, diseases, infections, trauma or injuries, tumors, osteotomies, and large fractures [2]. Typically, small bone defects heal spontaneously; however, the tissue's ability to heal is limited in massive defects; therefore, surgical intervention is required [3].

The mandible is one of the most structurally and functionally complex bones. It is essential for the aesthetic appeal of animal and human faces as well as many physiological functions, such as mastication and swallowing [4]. Critical sized mandibular defects may cause severe facial deformities, along with lingual and masticatory dysfunctions.

Therefore, reconstruction and repair of mandibular defects are significant issues in plastic and maxillofacial surgery [4–6]. Therefore, bone grafts play a significant role and are required to reconstruct large bone defects [7]. Autografts, allografts, xenografts, and synthetic bone graft substitute materials (alloplastic) have been reported [8].

Autografts refer to bone grafting from one site to another within the same animal, whereas allografts involve grafting from one animal to another of the same species [9]. Xenografts involve grafting from one animal to another of a different species [10]. Osteogenesis, osteoconduction, osteoinduction, and osteointegration are biological properties required to form new bone [11]. Autografts satisfy these requirements; consequently, they are regarded as the gold standard for treating bone defects [10]. There are limitations associated with the use of autografts and allografts [11,12]. Both xenogenic bone grafts and tissue engineering materials with enhanced properties can be used to overcome these limitations [13]. Bone-derived xenografts are widely used in maxillofacial applications [14].

MPM is an autologous blood product highly concentrated in platelets and fibrin in liquid form and combined with bone powder or bone substitute [12]. It is the most recent development in platelet concentrates and is a variant of platelet-rich fibrin [15]. Platelet concentrates are considered a suitable bioactive material because they provide an autologous source of growth factors and healing cytokines [16,17]. Moreover, fibrin is a biological material that provides an attractive scaffold that promotes cell migration, proliferation, and angiogenesis [18]. MPM offers additional advantages over platelet concentrates, such as incorporating bone graft particles into the fibrin network to produce sticky bone. The sticky bone is flexible and easy to shape, providing excellent stability to the bone particles and preventing the occupation of the defect site by soft tissue [15].

In orthopedic tissue engineering and regeneration, numerous natural and synthetic materials are used to form scaffolds that facilitate and accelerate the healing process of various tissues. Chitosan is a natural polymer widely used in the reconstruction and regeneration of bone [12]. Chitosan is an efficient, inexpensive biomaterial extracted from the shell of crustaceans. It is constituted mainly form N-acetyl D-glucosamine, which is one of the major constituents of the mammalian extracellular matrix (ECM). Chitosan can be further processed into various derivatives and various forms such as powders, flakes, membranes, sponges, fibers, and hydrogels. Due to this advantage, chitosan and its derivatives can be processed for various biological and biomedical application [19]. Previous studies have demonstrated that chitosan is non-toxic, biocompatible, non-immunogenic, and slowly biodegradable. It combines a unique set of beneficial properties for wound healing [11].

So far, there is no confined definition of a critical-sized defect. Generally, a critical-sized bone defect could be defined as an intraosseous defect that would not heal spontaneously without surgical stabilization, and requires further surgical intervention [20,21]. Therefore, our study aimed to evaluate the impact of MPM and Chitosan on the healing of a surgically-induced critical-sized mandibular bone defect (1 cm in diameter) in a rabbit model.

2. Materials and Methods

2.1. Ethical Approval

All the procedures and protocols involved in both welfare and surgical techniques of this study were reviewed by The Research Ethics Committee of the Faculty of Veterinary Medicine at Kafrelsheikh University, under approval number KFS-2021/5.

2.2. Animals

This study used 45 skeletally mature white adults New Zealand rabbits, weighing 3 ± 0.25 kg and aged 5–6 months. Rabbits were housed separately in a battery cage system depending on the natural lighting system at 21–28 °C. Rabbits had unrestricted access to commercially available, complete rabbit diets (Ibex International Co., Ltd., Nubaria, Egypt) and clean tap water. Before the surgery, 2 weeks were allotted for adaptation and observation [22].

2.3. Animal Grouping

The animals were randomly divided into three groups (n = 15) based on the filling material as shown in Figure 1A.

(a) Control group (C): the defect was filled with sterile saline solution (Otsuka, Japan).
(b) Chitosan group (Ch): the defect was filled by chitosan.

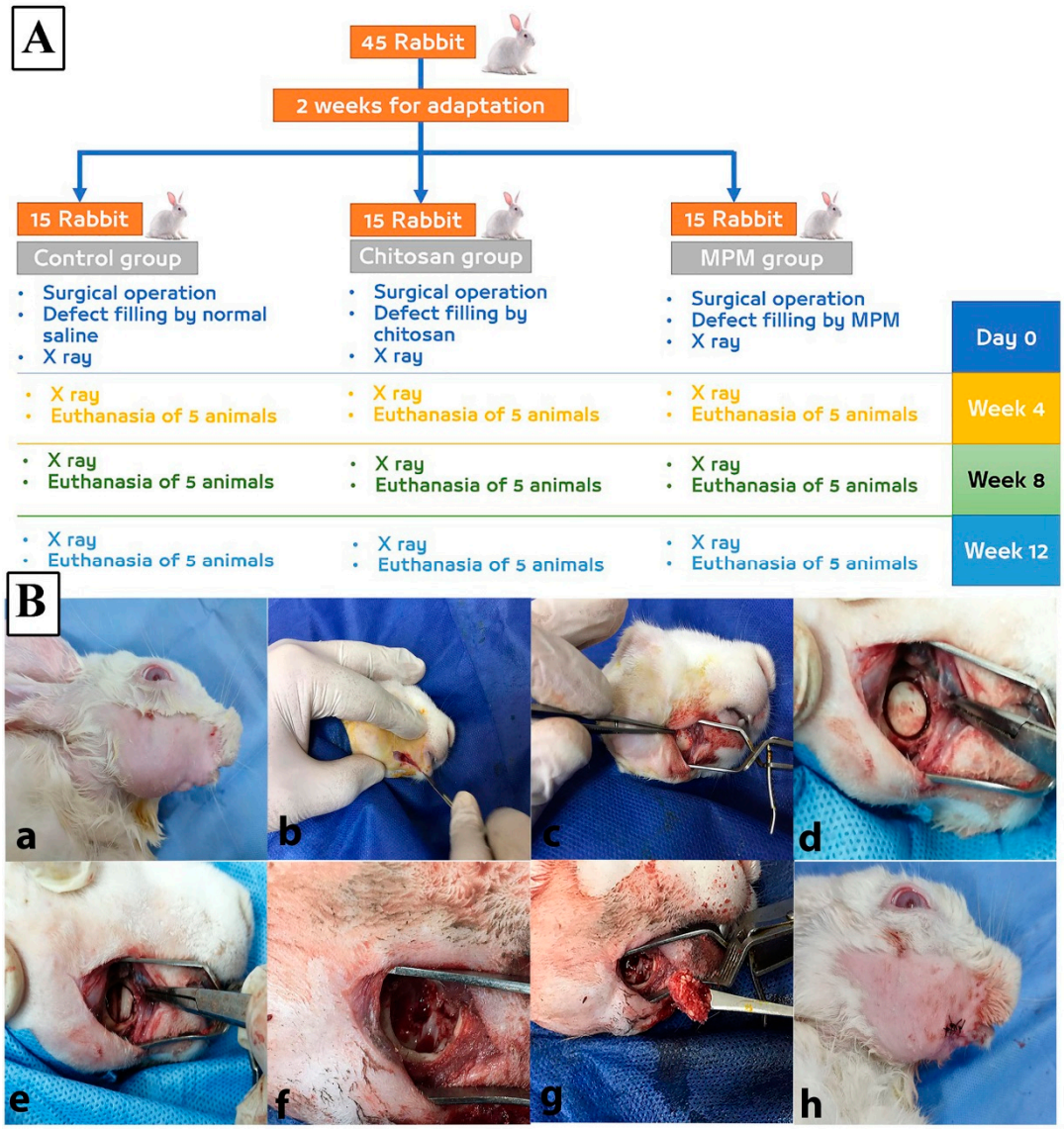

Figure 1. (**A**) Illustrative diagram of the experimental animal protocol. (**B**) Surgical procedures performed included the following: (**a**) preparation of the premolar molar area of the rabbit mandible, (**b**) incision of the skin, (**c**) dissection and exposure of the mandible, (**d**) demarcation of the defect circle by 10 mm trephine bur, (**e**) removal of marked 10 mm diameter cortical bone and exposure of teeth roots, (**f**) completing the defect till 10 mm width and removal of teeth roots by rose head bur, (**g**) filling materials are added to the defect area, and (**h**) suturing of musculature, subcutaneous tissue, and skin is undertaken.

According to Shah et al. [23], chitosan has a medium molecular weight of 300 kDa, with a deacetylation degree of 75 ± 10%, (Chitosan Egypt, Giza, Egypt). Ch was dissolved in acetic acid, followed by the addition of glutaraldehyde. The mixture was homogenized, frozen, lyophilized, sterilized, and packaged.

(c) MPM group: defect was filled by MPM.

The MPM was prepared by withdrawing 5 mL of venous blood from the ear vein and centrifuging it at 2700 rpm for 4 min. Plasma was collected using a sterile syringe and added to a sterile cup containing bovine corticocancellous bone granules (BMrebone 1H, UBGEN, Vignosa (PD), (Padova) Italy). Subsequently, the mixture was combined for 4 min to produce sticky bone (MPM) [24].

2.4. Surgical Procedures

Intramuscular injections of 5 mg/kg bwt xylazine hydrochloride (Xylaject, Adwia, New Cairo, Egypt) and 40 mg/kg bwt ketamine hydrochloride (Ketamine, Sigma, Cairo, Egypt) were used to induce anesthesia in rabbits [25,26]. The right mandible of each animal was prepped for aseptic surgical intervention. Along the lateral side of the rabbit mandible at the level of the first and second premolar teeth, as shown in Figure 1B, a skin incision was made. The skin incision was made 2–3 mm dorsal to the ventral border of the mandible [23]. Fascia and muscles were meticulously dissected to expose the mandible while avoiding the facial artery. After exposure of the mandible, a 10 mm diameter, 3 mm depth defect was made by using a micro-motor (STRONG 207 B, SAESHIN PRECISION Co., Ltd., Deagu, Korea) with contra-angle low speed (STRONG ACL (B)-01C SAESHIN PRECISION Co., Ltd., Deagu, Korea) and 10 mm diameter trephine bur followed by rose head bur under continuous irrigation with normal saline [27]. According to the group of the animals, different filling materials were used to fill the defect. The muscle and subcutis were sutured by simple continuous pattern using 4-0 polyglycolic acid sutures (SURGICRYL-PGA, SMI AG, Vith., Belgium), followed by suturing of the skin by simple interrupted suture pattern using 2-0 polyglycolic acid sutures (SURGICRYL-PGA, SMI AG, Vith., Belgium [22].

2.5. Clinical Evaluation

Postoperatively, animals in all three groups were injected with 10,000 IU/kg bwt of penicillin and 10 mg/kg bwt of streptomycin (Pen & Strep Norbrook, West Sussex, RH15 0DQ, UK) with a single dose per day subcutaneously (S/C) for 5 consecutive days [22]. To determine the presence of any infection, wound dehiscence, edema, or abnormalities, animals were kept under observation. Daily clinical evaluations of body temperature, food intake, body weight, and activity were conducted for the first 30 days following surgery [28]. The animals were then evaluated weekly throughout the study for feed intake and body weight.

2.5.1. Radiography and Radiographic Scoring

Plain film radiography was performed using the X-ray apparatus (GXR 52 S, DRGEM Co., Ltd., Seoul, Korea) with CR system (FUJIFILM-FCR PRIMA II. FUJIFILM UK Ltd., Bedford, UK). The X-ray beam was applied with the following parameters: 70 KV for 0.32 s and 10 mA. X-rays were taken postoperatively at 0, 4, 8, and 12 weeks [29]. The grading system described by Al-Fotawei et al. [29] was used to assess the quality and quantity of radiographic bone development. It involves six grades; Grade 0 denotes no change in the size and contour of the surgical defect from its immediate postoperative appearance after surgery. In Grade 1, the surgical defect contains traces of radio-dense materials. Grade 2 is defined as flocculent radiodensity with calcification particles. Grade 3 defects are bridged at least once with radio-dense material. In grade 4, the defect is filled with a substance of uniform radiodensity rostrally and caudally, although the ends of the cortices remain visible. Grade 5 is similar to grade 3, but newly formed radio-opaque tissue obscures at least one cortex. A surgical defect of grade 6 is completely indistinguishable from the surrounding bony edge and is bridged by homogeneous radiopaque tissue. Two blind radiologists independently evaluated the radiographic images.

2.5.2. Histopathology

Five animals from each group were euthanized using thiopental sodium anesthesia overdose at 4, 8, and 12 weeks after surgery. Five specimens per group (one per animal)

were histologically examined with H&E stain and Masson's trichrome stains [30]. Emery's histological scoring system classified histopathological findings into 7 grades. Grade 0 denotes no effect; grade 1 denotes only fibrous tissue in the defect area; grade 2 denotes more fibrous tissue than fibrocartilage; grade 3 denotes more fibrocartilage than fibrous tissue; grade 4 denotes only fibrocartilage; grade 5 denotes more fibrocartilage than bone; grade 6 denotes more bone than fibrocartilage; and grade 7 denotes only bone [31].

2.5.3. Immunohistochemical Procedures

The immunohistochemical techniques were performed in accordance with Abdo et al. [32]. For antigen retrieval, the tissues were fixed on charged slides, dewaxed, and immersed in a 0.05 M solution of citrate buffer, pH 6.8. The sections were then submerged in a 0.3% H_2O_2 solution to inhibit the nonspecific reaction. The sections were then incubated with the following primary antibodies: Rabbit polyclonal anti-NF-kB P65 (Santa Cruz, Cat# (F-6): sc-8008, 1:100 dilution) and MMP-9 antibody (Abcam, Cat# ab119906, Cambridge, MA, USA). After 12 h, the slides were rinsed in phosphate-buffered saline and incubated for 30 min at room temperature with a goat anti-rabbit secondary antibody (Cat# K4003, EnVision+™ System Horseradish Peroxidase Labeled Polymer; Dako). Tissues were visualized using a DAB kit and counter-stained with Mayer's hematoxylin. ImageJ analysis software determined the intensity of the staining and presented it as a percentage of positive area per mm^2.

2.6. Statistical Analysis

The data were analyzed using GraphPad Prism 6 statistical software (GraphPrism Software, La Jolla, CA, USA). In order to determine statistical significance between groups, a one-way analysis of variance (ANOVA) with the nonparametric Kruskal–Wallis H test, followed by Dunn's multiple comparison test, was employed. When the p-value was less than 0.05, significance was determined [22].

3. Results

3.1. Clinical Findings

All surgical procedures were completed without any intraoperative complications. Five rabbits exhibited minor post-operative swelling at the surgical site for 3 days, after which they recovered spontaneously. All animals experienced appetite loss and decreased food intake, which returned to normal within 5–7 days. Throughout the study, no signs of infection, debility, or loss of mandibular function were observed.

3.2. Radiographic Findings

Radiographic images and scoring at weeks 4, 8, and 12 post-operation are presented in Figures 2 and 3.

In the fourth post-operative week, animals in the control group demonstrated a lesser degree of bone formation with the appearance of radiopaque areas of new bone formation at the margins of the defect without evidence of bridging the defect area. In the chitosan group, bridging of the defect area was noticed with more obvious bone formation than the control one. The MPM group demonstrated more pronounced bone formation.

The chitosan and control groups differed significantly ($p = 0.0002$), so did the MPM group and the control group ($p = 0.0004$). Conversely, there was no statistically significant difference between the MPM group and the chitosan group ($p = 0.1194$).

In the 8th week following surgery, all three groups demonstrated an increase in bone formation to varying degrees. MPM group demonstrated the most pronounced bone formation with the greatest increase in defect area radio-opacity. The chitosan group exhibited a significant increase in bone formation and radio-opacity but to a lesser degree than the chitosan group.

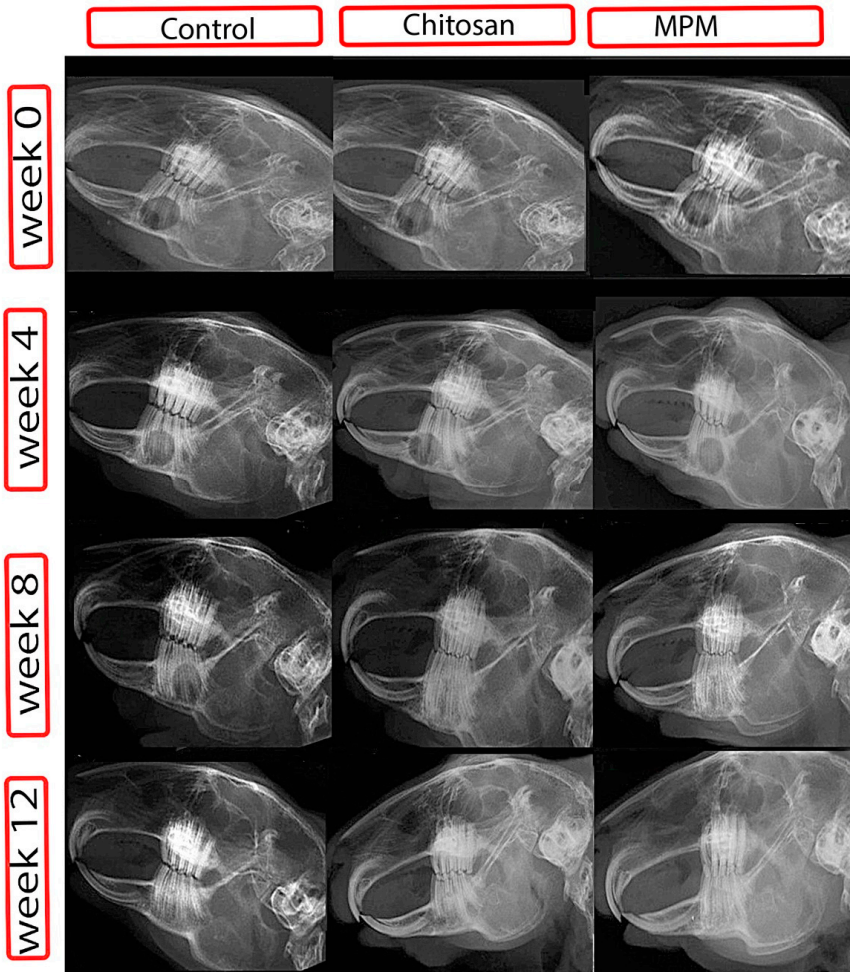

Figure 2. Lateral images of the skull at various times (0, 4, 8, and 12 weeks). At week 0, all animals display a radiolucent circular area representing the defect in all animals. At 4 and 8 weeks, MPM group demonstrated the most pronounced bone formation with the greatest increase in defect area radio-opacity as compared to chitosan and control groups. At the end of 12 weeks, MPM group demonstrated the highest degree of bone formation with uniform radio-opacity, while in the chitosan group, most of the defect area was filled with radio-opaque bone with persistent small radiolucent areas. The control group showed less bone formation than the MPM and chitosan group, with more radiolucent areas.

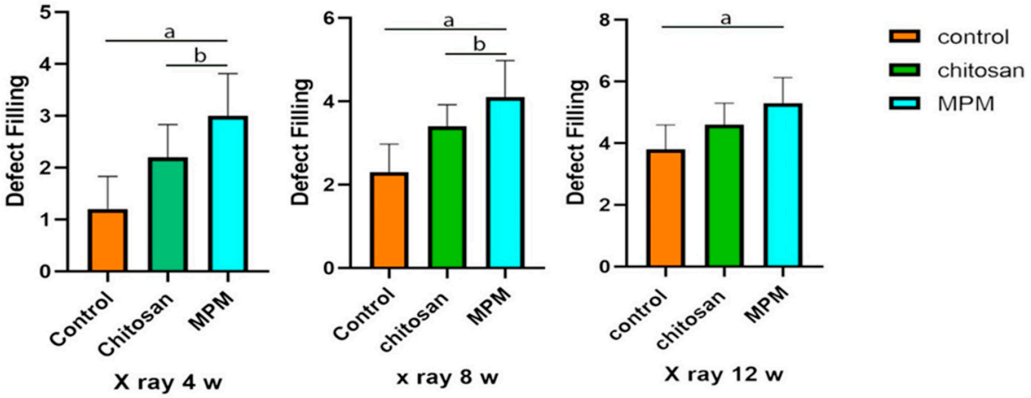

Figure 3. Depicts X-ray statistics at 4, 8, and 12 weeks postoperatively. The data were expressed as the mean ± SD. Superscript letters indicate the significance level; "a" refers to the significant difference

between the MPM and the control groups; "b" refers to the significant difference between the MPM and Chitosan groups ($p < 0.05$). At 4 and 8 weeks, a significant difference was observed between the chitosan group and the control group, as well as the MPM group and the control group. At 12 weeks, a significant difference was observed only between the MPM and the control groups.

The chitosan group and the control group differed significantly ($p = 0.0082$), so did the MPM group and the control group ($p = 0.0019$). However, there was no discernible difference between the MPM and chitosan groups ($p = 0.1017$).

At the end of the 12th post-operative week, the MPM group demonstrated the highest degree of bone formation with uniform radio-opacity nearly identical to that of adjacent healthy parent tissue. While in the chitosan group, most of the defect area was filled with radio-opaque bone with persistent small radiolucent areas. The control group showed less bone formation than the MPM and chitosan group, with more radiolucent areas.

At the conclusion of the study, there was no statistically significant difference between the chitosan group and the control group ($p = 0.0851$) or between the MPM group and the chitosan group ($p = 0.2735$). Interestingly, a significant difference was observed between the MPM group and the control group ($p = 0.0044$), indicating that MPM has a promising effect on bone formation and remodeling.

The evaluation of radiographic findings at 4, 8, and 12 weeks postoperatively revealed that the control group displayed variable bone formation at the defect margin without extension into the defect center. In the chitosan group, the defect was filled with newly formed bone. Intriguingly, the MPM group's defect area was filled with radiopaque bone that resembled the parent bone.

In the 12th post-operative week, the MPM group demonstrated superior integration of the newly formed bone with the parent bone compared to the chitosan group.

3.3. Histological Findings

3.3.1. H&E-Staining

In the 4th post-operative week, inflammatory reaction and hematomas were still evident in the control group but significantly diminished in the MPM group as illustrated in Figure 4. Granulation tissue formation was pronounced in the MPM and chitosan groups but less pronounced and still distinct in the control group. Intriguingly, the MPM revealed a significant increase in the formation of granulation tissue and osseous tissue.

Regarding the findings noticed at the 8th post-operative week, the defect area of the control group was filled with granulation tissue with the formation of unconnected osseous tissue (islets). The process of angiogenesis was still active. In addition to similar results, the defect area in the chitosan group demonstrated increased osteoplastic cell proliferation, osteoid matrix, and osteogenesis. The MPM group's defect area indicated the presence of bone powder surrounded by a matrix resembling dentine, along with marked odontoblastic, osteoplastic cell proliferation, and marked osteogenesis (Figure 5).

In the 12th week after surgery, defect areas in the control group exhibited ossification, but the remodeling was not evident. The presence of immature granulation tissue was observed alongside minute hematomas. Defect areas in the chitosan group exhibited an incomplete Haversian system with mature fibrous connective tissue formation and a small amount of granulation tissue. Defect areas in the MPM group exhibited complete remodeling, as evidenced by the presence of MPM spicules in the bone matrix and a pronounced presence of osteocytes (Figure 6).

The histopathology score was illustrated in Figure 7; at the 4th week, a significant difference between the MPM and control group was noticed ($p = 0.0019$). There was no significant difference between the chitosan and the control groups ($p = 0.2881$). At the 8th week, a significant difference between the MPM group and the control group ($p = 0.0034$) as well as between the MPM group and the chitosan group was observed ($p = 0.0262$). At the 12th week, a significant increase of the healing score between MPM and control group was detected ($p = 0.0005$).

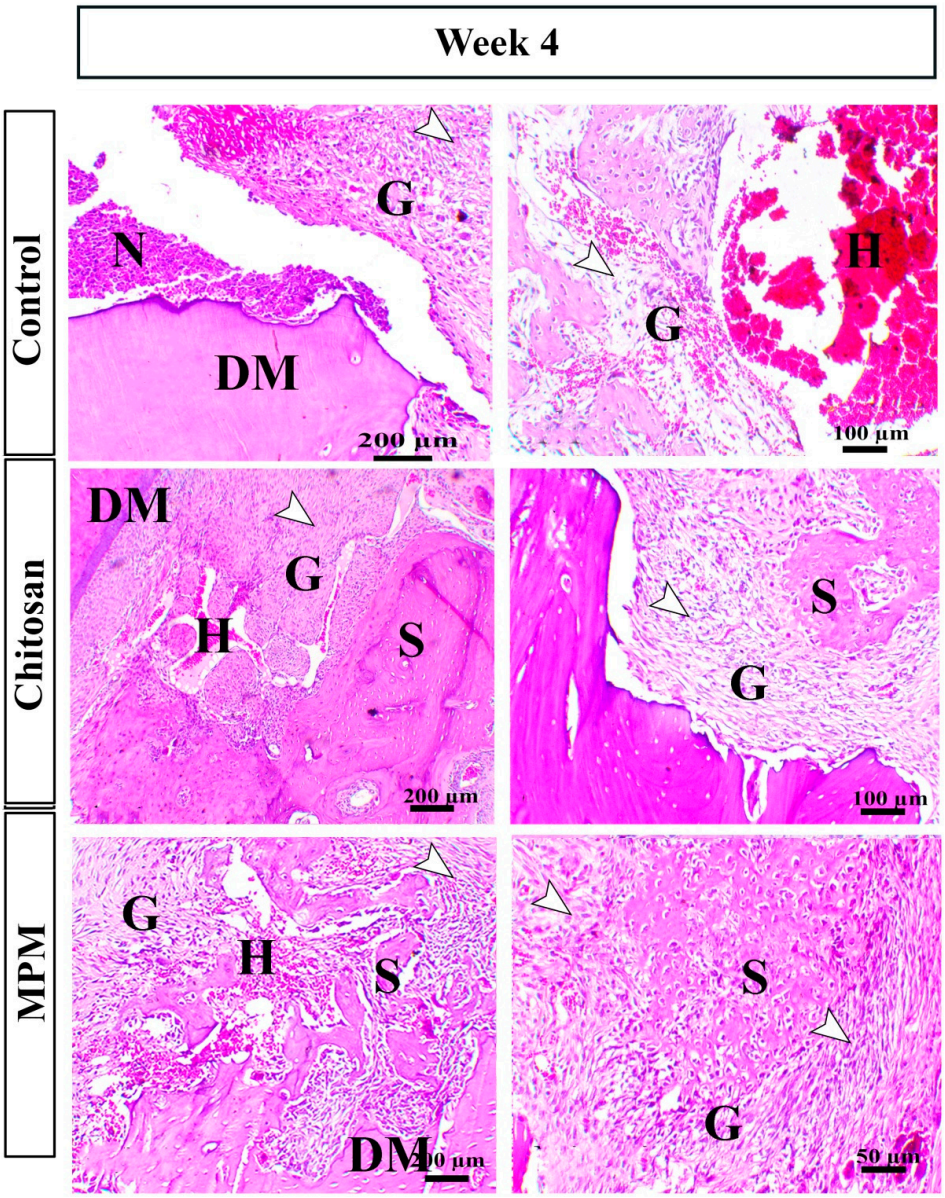

Figure 4. Photomicrographs of various H&E-stained bone sections from the three groups at the 4th week postoperatively. G represents granulation tissue, S represents osseous tissue, H indicates hemorrhage, DM indicates defect margin, and arrowheads indicate fibroblastic cells.

3.3.2. Masson's Trichrome Staining

Evaluation of collagen fiber deposition at the 4th postoperative week showed that the MPM and chitosan groups demonstrated early collagen fiber deposition, either interstitial or within the newly formed osseous tissue (Figure 8). Quantitative scoring of collagen deposition showed significant increases in collagen deposition between MPM and the control group (p = 0.0005), chitosan and the control group (p = 0.0011), and MPM and chitosan (p = 0.0039). During the 8th postoperative week, both the MPM and chitosan groups demonstrated a remarkable increase in collagen deposition within the defect area. Significant increases in collagen deposition were observed between MPM and the control group (p = 0.0002), chitosan and the control group (p = 0.0023), and MPM and Chitosan (p = 0.0039) (Figure 9). At the 12th postoperative week, the MPM showed deposition of well-organized and abundant collagen fibers (Figure 8). Collagen deposition increased

significantly between MPM and the control group (p = 0.0001), chitosan and the control group (p = 0.0003), and between MPM and chitosan (p = 0.0157) (Figure 9).

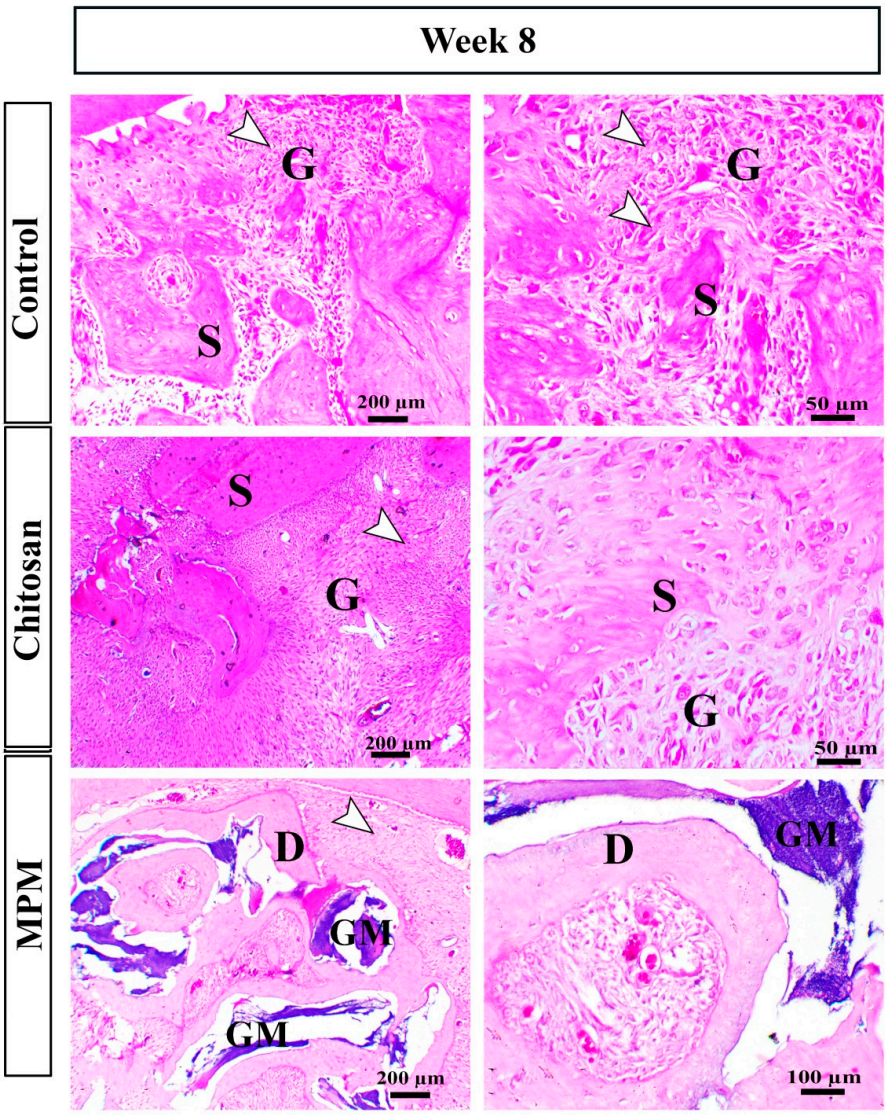

Figure 5. Photomicrographs of various H&E-stained bone sections from the three groups at the 8th week postoperatively. G represents granulation tissue, S represents osseous tissue, H indicates hemorrhage, D indicates dentin-like material, GM indicates MPM graft material, and arrowheads indicate fibroblastic cells.

3.4. Immunohistochemical Findings

3.4.1. Nuclear Factor Immune Staining (NF-κB (P65))

NF-κB (p65) IHC was demonstrated in Figures 10 and 11. Both the MPM and chitosan groups expressed less NF-κB (p65) than the control group in the 4th week following surgery. Expression of NF-κB (p65) decreased significantly in the MPM group in comparison with the control group (p = 0.0003), chitosan and the control group (p = 0.0005), and between MPM and chitosan (p = 0.0039). Both MPM and chitosan groups demonstrated a significant decrease in NF-κB (p65) expression within the defect area during the 8th week following surgery. The expression of NF-κB (p65) decreased significantly between MPM and the control group (p = 0.0002), chitosan and the control group (p = 0.0020), and between MPM and chitosan (p = 0.0001). In the 12th post-operative week, both treated groups continued to exhibit decreased expression compared to the control group. The expression of NF-κB

(p65) was significantly different between MPM and the control group ($p = 0.0001$), chitosan and the control group ($p = 0.0001$), and MPM and chitosan groups ($p = 0.0005$).

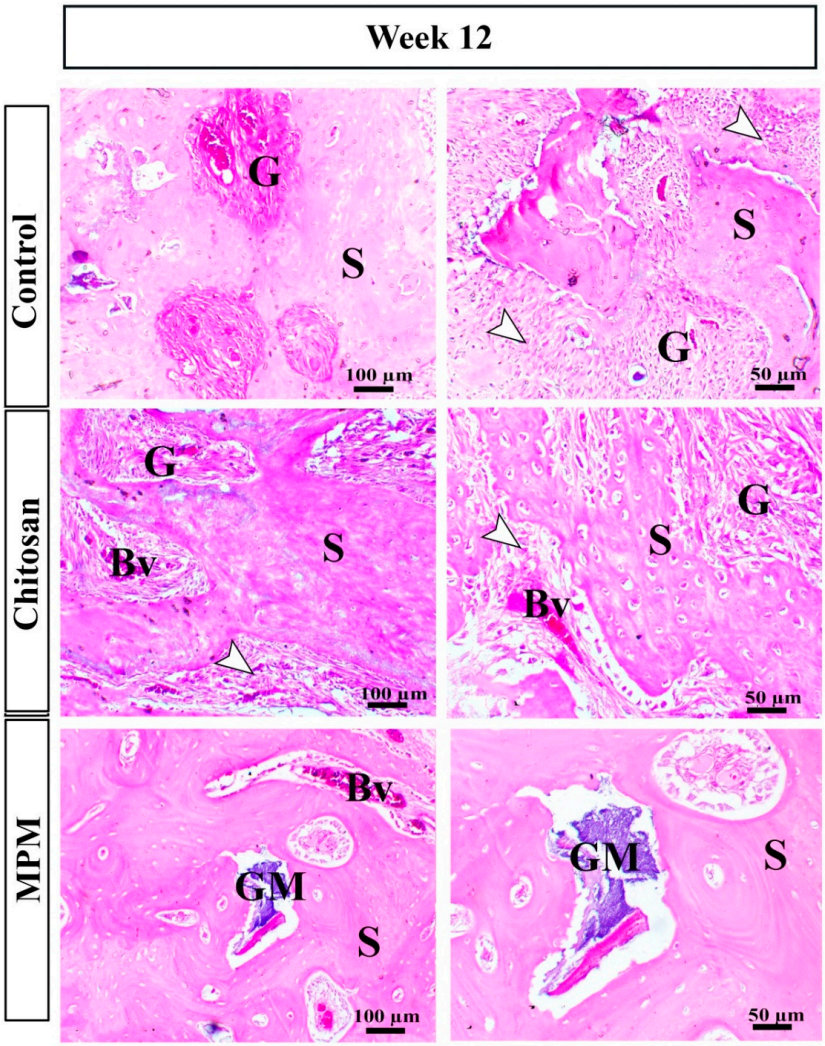

Figure 6. Photomicrographs of various H&E-stained bone sections from the three groups at the 12th week postoperatively. G represents granulation tissue, S represents osseous tissue, Bv denotes blood vessel, H indicates hemorrhage, D indicates dentin-like material, GM indicates MPM graft material, and arrowheads indicate fibroblastic cells.

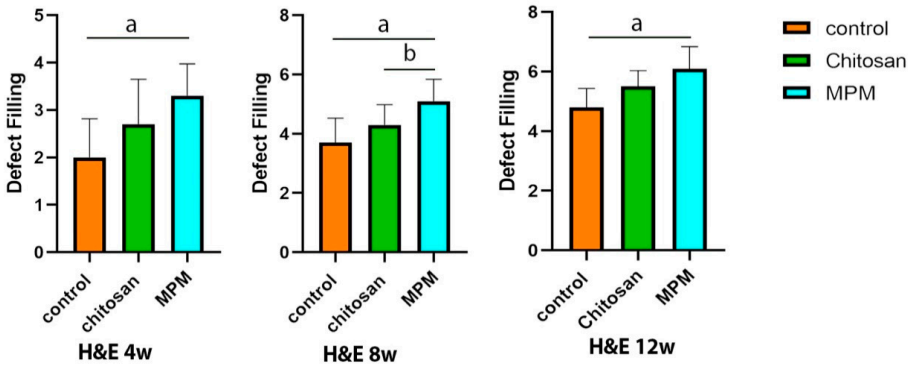

Figure 7. H&E-stained bone section statistics at 4, 8, and 12 weeks postoperatively. The data were expressed as a mean ± standard deviation. "a" indicates a significant difference between the MPM and control groups; "b" indicates a significant difference between the MPM and chitosan groups ($p < 0.05$).

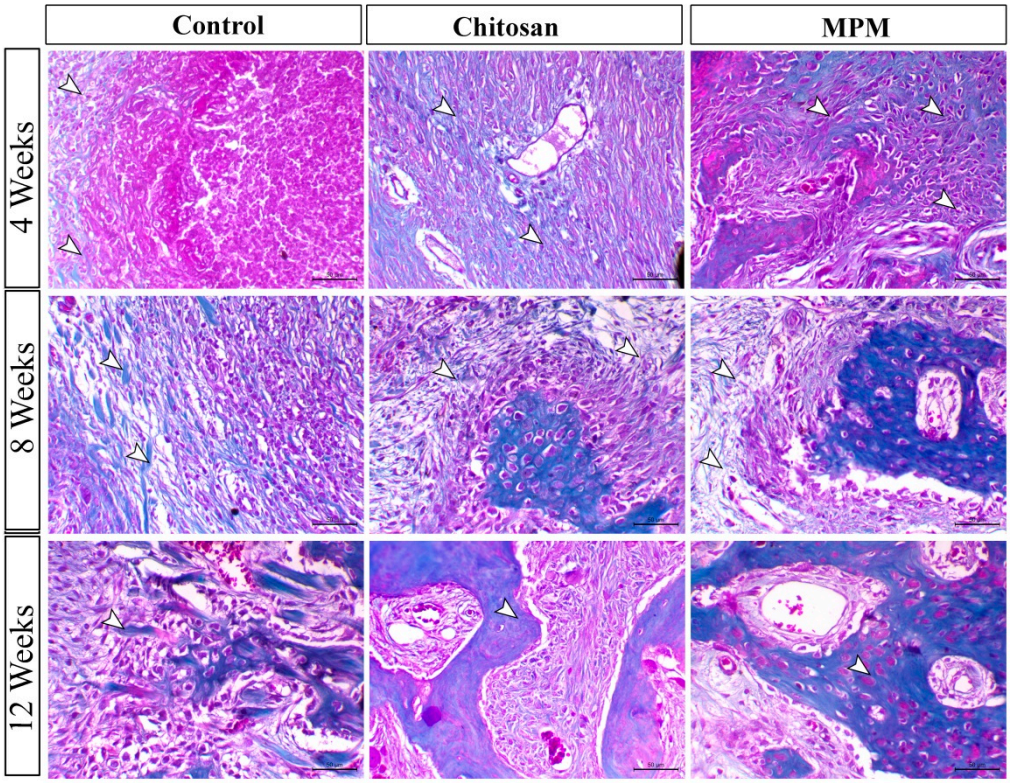

Figure 8. Photomicrographs of various trichrome-stained bone sections from the three groups at 4, 8, and 12 weeks postoperatively. Arrowheads represent collagen fibers, stained with Masson's Trichrome; bar = 50 µm.

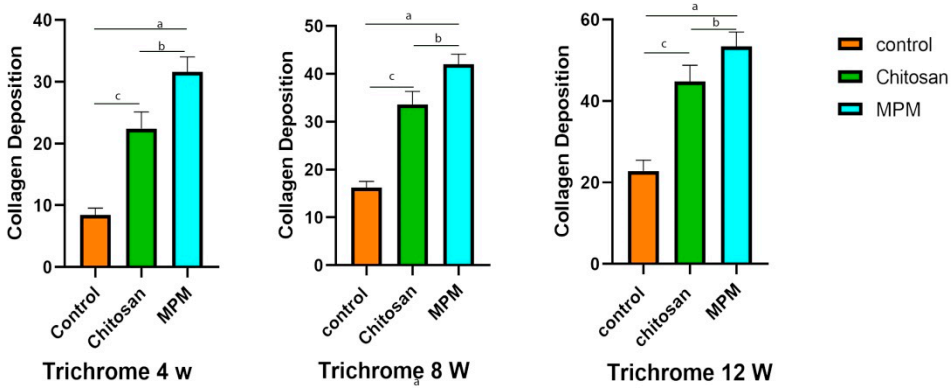

Figure 9. Quantitative scoring of collagen deposition between the different groups. The data are expressed as mean ± standard deviation. SD. Superscript letters indicate the significance level; "a" refers to the significant difference between the MPM and the control groups; "b" refers to a significant difference between MPM and chitosan groups; and "c" refers to the significant difference between the Chitosan and control groups ($p < 0.05$).

3.4.2. Matrix Metalloproteinase-9 Immune Staining

The illustrative photomicrograph and the quantitative chart of MMP9 were illustrated in Figures 12 and 13. In the control group, the MPM and chitosan groups showed a significant increase in MMP-9 expression in the 4th week following surgery. MMP-9 expression increased significantly between MPM and the control group ($p = 0.0001$), chitosan and the control group ($p = 0.0006$), and between MPM and chitosan ($p = 0.0021$). Both the MPM and chitosan groups demonstrated a remarkable increase in MMP-9 expression in the defect area during the 8th week following surgery. MMP-9 expression increased significantly be-

tween MPM and the control group (p = 0.0001), chitosan and the control group (p = 0.0001), and between MPM and chitosan (p = 0.0001).

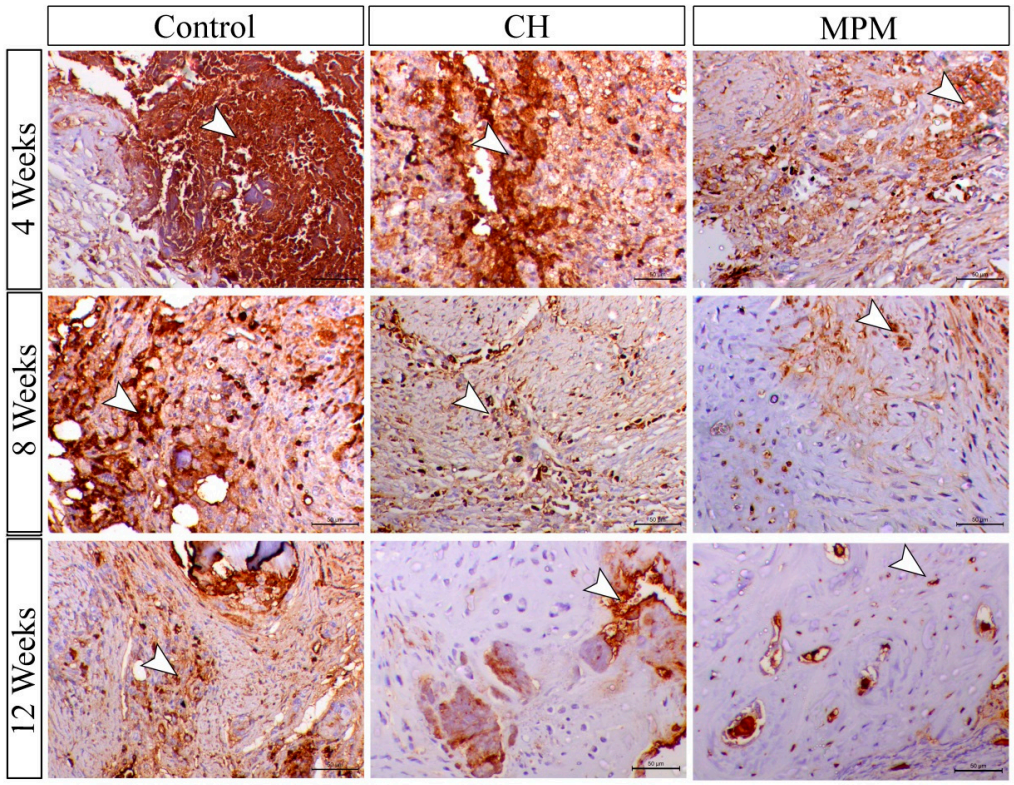

Figure 10. Different NF-κB (p65) IHC-stained bone sections of the three groups at 4, 8, and 12 weeks postoperatively. The arrowheads represent positive expression, and the bar represents 50 μm.

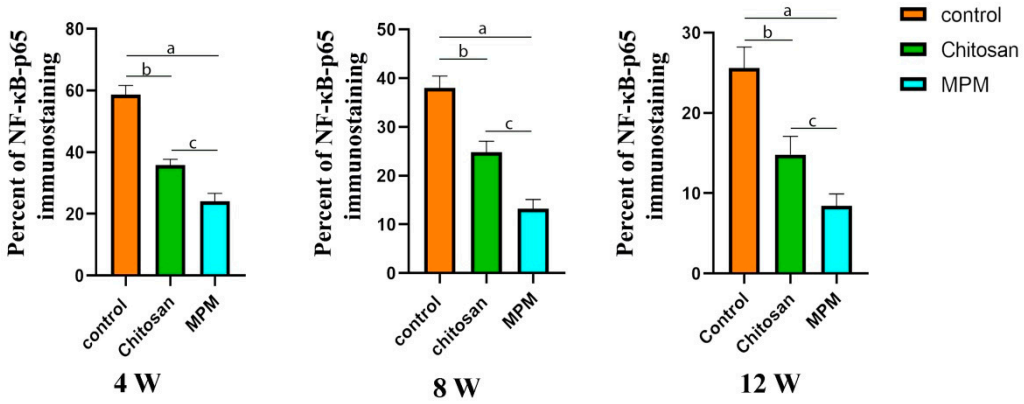

Figure 11. Quantitative scoring of NF-κB (p65) IHC-stained mandibular bone sections of the three groups at 4, 8, and 12 weeks postoperatively. The data are expressed as mean ± SD. Superscript letters indicate the significance level; "a" refers to the significant difference between the MPM and the control groups; "b" refers to a significant difference between chitosan and control groups; and "c" refers to the significant difference between the MPM and Chitosan groups ($p < 0.05$).

During the 12th week postoperatively, both treated groups continued to exhibit elevated expression compared to the control group. MMP-9 expression increased significantly between MPM and the control group (p = 0.0001), chitosan and the control group (p = 0.0017), and between MPM and chitosan (p = 0.0004).

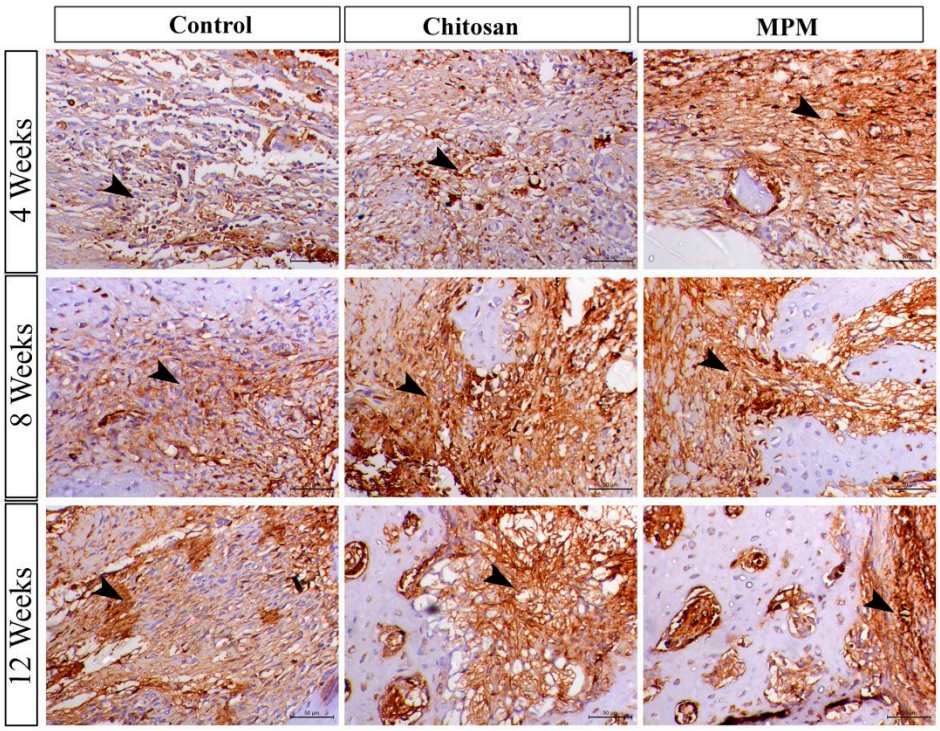

Figure 12. Photographs of various MMP-9 IHC-stained bone sections from the three groups at 4, 8, and 12 weeks postoperatively. The arrowheads represent positive expression, and the bar represents 50 µm.

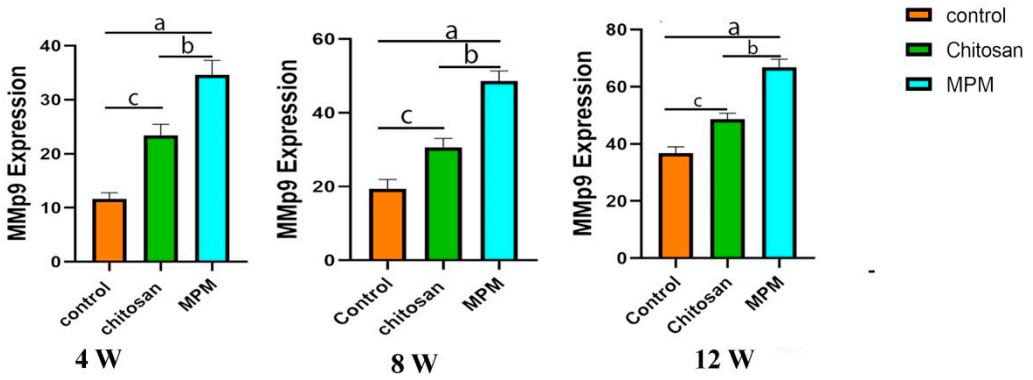

Figure 13. Quantitative scoring of NF-κB (p65) IHC-stained bone sections of the three groups at 4, 8, and 12 weeks postoperatively. The data are expressed as mean ± SD. Superscript letters indicate the significance level, where "a" refers to the significant difference between the MPM and the control groups, "b" refers to a significant difference between the MPM and chitosan groups, and "c" refers to the significant difference between the Chitosan and control groups ($p < 0.05$).

4. Discussion

Repair of large segments of bone defects is a major issue in oral and maxillofacial surgery [33]. It necessitates intricate and essential interactions between cells, growth factors, and scaffolding materials [34]. In our study, we used a rabbit model. Rabbit has been tremendously used in bone studies. It has numerous advantages such as complete bone maturity at 6 months, rapid intracortical and Haversian remodeling, and fast bone regeneration in 30 days. The size of the mandibular defect was performed in accordance to Vasilis Thomaidis [35]. Schmitz et.al reported that a critical non-spontaneous bone defect could be established by a diameter of more than 5 mm [36]. Our treatment protocol

excludes anti-inflammatory agents, to avoid their possible interaction with the tested graft materials, as some anti-inflammatory agents may accelerate or retard bone healing [22].

The present study was aimed at evaluating the use of Chitosan and MPM for treating large mandibular bone defects. It has been documented that chitosan preparations are used in mandibular bone defects either alone or in conjunction with other materials or cells [37], whereas MPM usage was restricted to periodontology.

Although the creation of mandibular bone defects of critical size in rodents without tooth extraction increases the risk of infection and avascular necrosis [38], the current results indicate that neither the MPM nor the chitosan groups got infected. Numerous studies have reported that Chitosan possesses antimicrobial activity [39], and we strongly suggest that MPM plays a role in preventing infection at the defect site, though further research is required on this point. Five animals in the control group, two in the chitosan group, and only one in the MPM group exhibited radiolucent areas around the tooth roots, indicating periapical lesions. Periapical lesions may be caused by different etiological agents of endodontic origin. Many issues can result in apical periodontitis, for example: poor aseptic measurements, inadequate access cavity design, missed canals, insufficient instrumentation, debridement, and leaking temporary or permanent restorations. Even when the strictest precautions are taken, apical periodontitis may still persist as asymptomatic radiolucencies, because of the complexity of the root canal system formed by the main and accessory canals. Additionally, the inflammatory periapical tissue contains extra radicular causes that may prevent post-treatment recovery [40].

The MPM group displayed the most radio-opacity at the defect site, whereas the control group displayed the least radio-opacity, indicating a lower degree of osseous tissue formation than both treated groups. This demonstrates the favorable effect of MPM on bone formation and remodeling consistent with the positive radiographic effects of MPM reported by Amine et al. [41], who used MPM to augment the volume of the socket bone prior to dental implant placement.

The radiographic findings were confirmed histologically, and enhanced bone regeneration was observed in the MPM and chitosan groups. In contrast to the MPM and chitosan groups, the control group continued to exhibit inflammatory cell infiltration through the 8th week of the study. Both treated groups had a greater number of fibroblasts, newly formed blood vessels, and osteogenic cells that produced more woven bone. The MPM group had a more mature cancellous bone than lamellar bone, with a well-developed marrow cavity at the conclusion of the study.

Our findings concur with Elmoheb et al. [42], who declared that MPM effectively induced bone formation. Soodeh et al. [23] reported that xenogenic demineralized bone matrix (DBM) and autografts have superior osteoinductive and osteoconductive properties to chitosan. These findings confirm the superior effect of MPM in enhancing new bone formation and remodeling and confirm our radiographic and histopathological results.

The inflammatory phase of bone healing requires the coordinated activation of distinct signaling pathways that regulate the expression of pro-and anti-inflammatory mediators in resident tissue cells and recruited leukocytes [43]. Nuclear factor kappa (NF-κB) is a cell-surface cytokine that is normally expressed by osteocytes and osteoblasts. It plays a crucial role in regulating the transcription of numerous inflammatory mediators [44]. In a particular setting, it aids in the resolution of inflammation [38]. The five subunits of NF-κB are p50, p65, rel A, Rel B, and c-rel [45]. During the acute phase of inflammation, NF-κB is activated, particularly the p50/p65 subunits, which induce transcription of pro-inflammatory mediators. During the inflammation resolution phase, p65 is degraded and removed from the nucleus [46]. At the end of the experiment, NF-κB (p65) was downregulated, according to our findings. This downregulation can be attributed to numerous factors, such as the secretion of osteoprotegerin (OPG) receptors by B cells, osteoblasts, and MSCs. OPG competes with nuclear factor ligand receptors (RANK) for binding with (RANKL), thereby decreasing the RANKL signaling pathway accountable for nuclear factor expression in activated T cells [47,48]. The plasma phase of MPM contains

many white blood cells, including B cells, which might explain why the expression of NF-κB (p65) was lower in the MPM group than in the chitosan and control groups. Overall, the downregulation of NF-κB (p65) indicates a decreased inflammatory response, reflecting the respective biocompatibility of MPM and chitosan.

Collagen fibers provide the filling material and scaffolding network for other growing cells, such as osteocytes and macrophages [49]. Fibrosis is a crucial step in bone healing. Collagen is the most structurally important protein in the bone extracellular matrix [49]. The deposition of collagen at the site of a bone fracture or defect indicates osteogenesis of mesenchymal stem cells (MSCs) [50]. Trichrome staining revealed that the MPM and chitosan groups deposited more collagen fibers than the control group throughout the experiment. According to Intini, 2009 [51], platelet-rich fibrin increases high-density bone formation through a significant increase in both type I collagen deposition and neovascularization [52]. Interestingly, we noticed the formation of dentin-like material within the histological features of MPM-treated animals, which may be due to the activation of osteoblastic and odontoblastic cells; especially dentine and bone tissue have many structural similarities. Therefore, dentine is considered a possible candidate for bone regeneration [53]. At the 12th week, dentin was markedly replaced with osseous matrix. Intriguingly, dentine matrices can stimulate osteogenesis and new bone formation by the stimulation of bone morphogenetic proteins (BMPs) [54].

Angiogenesis is essential for bone regeneration [55] to ensure the formation of new blood vessels (BVs) that increase the delivery of oxygen and nutrients necessary for osteogenesis [56]. In the early stages, hypoxia at the defect site induces activation of the NF-κB pathway [57], and induction of vascular endothelial growth factor (VEGF), which stimulates the chemotaxis and proliferation of endothelial cells (ECs), which then secrete local MMPs that degrade the extracellular matrix, thereby creating space for neoangiogenesis and restoring oxygen tension at the hypoxic site [55].

In bone tissue, matrix remodeling controls the growth, maturation, and regression of BVs involved in neovascularization [58–60]. MMP-9 was expressed in osteoblasts, osteoclasts, osteocytes, and bone marrow cells, indicating that it is a bone resorption enzyme [61,62]. MMP-9 is closely associated with bone remodeling and forming new bone between graft particles [61,62]. VEGF is associated with BMP-2 [63] upregulation. BMPs are essential for all stages of bone healing because they induce the differentiation of MSCs into chondrogenic and osteogenic cell lines and stimulate angiogenesis [64]. An increase in VEGF without adequate levels of other growth factors may not accelerate bone healing [65]. For bone healing, sustained release of growth factors is more beneficial [66]. The plasma phase of MPM ensures long-term osteoinduction via the slow release of high growth factor concentrations from platelets, while the mineral phase provides an osteoconductive scaffold for bone formation [24]. Thus, the MPM significantly contributed to the acceleration of wound healing.

Throughout the experiment, the MPM and Chitosan groups exhibited significantly higher levels of MMP-9 expression, indicative of a greater blood supply and improved bone formation and remodeling. Similar results were found in critical-size cranial defects in rats using sintered anorganic bone grafts [55]. Peak expression of MMP-9 and VEGF was observed at 30 days and remained higher in the treated group between 21 and 180 days. In our study, MMP-9 expression increased throughout the experiment time. Rocha et al. [48] stated that the change in MMP-9 expression may be attributed to the type, mechanism of action, and physicochemical properties of the bone substitute materials. As stated by P. Sivashankari and M. Prabaharan, chitosan can stimulate angiogenesis [39].

5. Conclusions

Our study aimed to assess the effect of mineralized plasmatic matrix and chitosan on the healing of a critical-sized mandibular bone defect at 4, 8, and 12 post-operative weeks. Our results showed that the mineralized plasmatic matrix and chitosan improved the healing of a critical-sized mandibular bone defect qualitatively and quantitatively

by increasing angiogenesis, collagen deposition, matrix metalloproteinase-9 expression, osseous tissue formation, and down-regulating NF-κB expression (p65). Therefore, future studies are required to assess the effect of the mineralized plasmatic matrix and chitosan on the healing of a critical-sized mandibular bone defect in large number of clinical cases.

Author Contributions: Conceptualization, A.H., A.A., W.A., A.A.E. and G.E.; methodology, A.H., A.A., A.A.E., W.A. and A.O.; software, A.H., A.A.E. and A.S.; validation, W.A., G.E., X.X. and A.A.E.; formal analysis, X.X. and G.E.; investigation, W.A., G.E., A.S. and A.O.; resources, A.H. and X.X.; data curation, A.A., A.H. and X.X.; writing—original draft preparation, A.H., A.A., A.A.E., W.A. and A.O.; writing—review and editing, A.A., A.A.E., W.A., G.E., A.O. and X.X.; visualization, G.E. and X.X.; supervision, G.E., A.A., A.S. and X.X.; project administration, X.X.; funding acquisition, A.H. and X.X. All authors have read and agreed to the published version of the manuscript.

Funding: This research received no external funding.

Institutional Review Board Statement: All the procedures and protocols involved in both welfare and surgical techniques of this study were reviewed by The Research Ethics Committee of the Faculty of Veterinary Medicine at Kafrelsheikh University, under approval number KFS-2021/5.

Informed Consent Statement: Not applicable.

Data Availability Statement: The data that support the findings of this study are available upon request from the corresponding author.

Conflicts of Interest: The authors declare no competing interest.

References

1. Dimitriou, R.; Jones, E.; McGonagle, D.; Giannoudis, P.V. Bone regeneration: Current concepts and future directions. *BMC Med.* **2011**, *9*, 66. [CrossRef] [PubMed]
2. Holban, A.M.; Grumezescu, A. *Materials for Biomedical Engineering: Hydrogels and Polymer-Based Scaffolds*; Elsevier: Amsterdam, The Netherlands, 2019.
3. Oryan, A.; Alidadi, S.; Moshiri, A.; Maffulli, N. Bone regenerative medicine: Classic options, novel strategies, and future directions. *J. Orthop. Surg. Res.* **2014**, *9*, 18. [CrossRef] [PubMed]
4. Wu, J.; Liu, J.; Wang, L.; Xie, A.; Liu, D. Bone histomorphometry detection of autologous bone powder graft repair of partial mandibular defects in rabbits. *Genet. Mol. Res.* **2015**, *14*, 13812–13822. [CrossRef] [PubMed]
5. Kumar, B.P.; Venkatesh, V.; Kumar, K.; Yadav, B.Y.; Mohan, S.R. Mandibular reconstruction: Overview. *J. Maxillofac. Oral Surg.* **2016**, *15*, 425–441. [CrossRef]
6. Zhang, Q.; Wu, W.; Qian, C.; Xiao, W.; Zhu, H.; Guo, J.; Meng, Z.; Zhu, J.; Ge, Z.; Cui, W. Advanced biomaterials for repairing and reconstruction of mandibular defects. *Mater. Sci. Eng. C* **2019**, *103*, 109858. [CrossRef]
7. Saikia, K.; Bhattacharya, T.; Bhuyan, S.; Talukdar, D.; Saikia, S.; Jitesh, P. Calcium phosphate ceramics as bone graft substitutes in filling bone tumor defects. *Indian J. Orthop.* **2008**, *42*, 169. [CrossRef]
8. Bauer, T.W.; Muschler, G.F. Bone graft materials: An overview of the basic science. *Clin. Orthop. Relat. Res.* **2000**, *371*, 10–27. [CrossRef]
9. Denny, H.; Butterworth, S. *A Guide to Canine and Feline Orthopaedic Surgery*; Wiley: Hoboken, NJ, USA, 2008.
10. Campana, V.; Milano, G.; Pagano, E.; Barba, M.; Cicione, C.; Salonna, G.; Lattanzi, W.; Logroscino, G. Bone substitutes in orthopaedic surgery: From basic science to clinical practice. *J. Mater. Sci. Mater. Med.* **2014**, *25*, 2445–2461. [CrossRef]
11. Zamiri, B.; Shahidi, S.; Eslaminejad, M.B.; Khoshzaban, A.; Gholami, M.; Bahramnejad, E.; Moghadasali, R.; Mardpour, S.; Aghdami, N. Reconstruction of human mandibular continuity defects with allogenic scaffold and autologous marrow mesenchymal stem cells. *J. Craniofacial Surg.* **2013**, *24*, 1292–1297. [CrossRef]
12. Moshiri, A.; Shahrezaee, M.; Shekarchi, B.; Oryan, A.; Azma, K. Three-dimensional porous gelapin–simvastatin scaffolds promoted bone defect healing in rabbits. *Calcif. Tissue Int.* **2015**, *96*, 552–564. [CrossRef]
13. Saravanan, S.; Leena, R.; Selvamurugan, N. Chitosan based biocomposite scaffolds for bone tissue engineering. *Int. J. Biol. Macromol.* **2016**, *93*, 1354–1365. [CrossRef] [PubMed]
14. Soares, M.Q.S.; Van Dessel, J.; Jacobs, R.; Yaedú, R.Y.F.; Sant'Ana, E.; da Silva Corrêa, D.; Madeira, M.F.C.; Duarte, M.A.H.; Rubira-Bullen, I.R.F. Morphometric evaluation of bone regeneration in segmental mandibular bone defects filled with bovine bone xenografts in a split-mouth rabbit model. *Int. J. Implant Dent.* **2019**, *5*, 32. [CrossRef] [PubMed]
15. Mohamed, E.M. The use of growth factors fibrin network to enhance architecture, mechanical and biological aspect of the graft particles. *Int. J. Prev. Clin. Dent. Res.* **2014**, *1*, 41–44.
16. Mudalal, M.; Zhou, Y. Biological additives and platelet concentrates for tissue engineering on regenerative dentistry basic Science and concise review. *Asian J. Pharm.* **2017**, *11*, 255–263.

17. Weibrich, G.; Kleis, W.K.; Hafner, G. Growth factor levels in the platelet-rich plasma produced by 2 different methods: Curasan-type PRP kit versus PCCS PRP system. *Int. J. Oral Maxillofac. Implant.* **2002**, *17*, 184–190.
18. Mehrabani, D.; Khodakaram-Tafti, A.; Shaterzadeh-Yazdi, H.; Zamiri, B.; Omidi, M. Comparison of the regenerative effect of adipose-derived stem cells, fibrin glue scaffold, and autologous bone graft in experimental mandibular defect in rabbit. *Dent. Traumatol.* **2018**, *34*, 413–420. [CrossRef]
19. Amirthalingam, S.; Rajendran, A.K.; Mani, P.; Rangasamy, J. Perspectives and Challenges of Using Chitosan in Various Biological Applications. *Chitosan Biomater. III* **2021**, *287*, 1–22.
20. Keating, J.F.; Simpson, A.; Robinson, C. The management of fractures with bone loss. *J. Bone Jt. Surg. Br. Vol.* **2005**, *87*, 142–150. [CrossRef]
21. Wang, W.; Yeung, K.W.K. Bone grafts and biomaterials substitutes for bone defect repair: A review. *Bioact. Mater.* **2017**, *2*, 224–247. [CrossRef]
22. Elgendy, M.; Elsayad, G.; Seleim, M.; Abdo, W.; Baty, R.S.; Elmahallawy, E.K.; Atiba, A. Flunixin Meglumine Enhanced Bone Fracture Healing in Rabbits Associated with Activation of Early Collagen Deposition and Enhancement of Vascular Endothelial Growth Factor Expression. *Animals* **2021**, *11*, 2834. [CrossRef]
23. Alidadi, S.; Oryan, A.; Bigham-Sadegh, A.; Moshiri, A. Comparative study on the healing potential of chitosan, polymethyl-methacrylate, and demineralized bone matrix in radial bone defects of rat. *Carbohydr. Polym.* **2017**, *166*, 236–248. [CrossRef] [PubMed]
24. Ghanem, M.A.; Sharara, A.A.; Sweedan, A.O.; Khalil, N.M. Evaluation of using mineralized plasmatic matrix in osseous regeneration (experimental and histomorphometric study on rabbits). *Alex. Dent. J.* **2018**, *43*, 53–59. [CrossRef]
25. Monir, A.; Mukaibo, T.; El-Aal, A.; Nodai, T.; Munemasa, T.; Kondo, Y.; Masaki, C.; El-Shair, M.A.; Matsuo, K.; Hosokawa, R. Local administration of HMGB-1 promotes bone regeneration on the critical-sized mandibular defects in rabbits. *Sci. Rep.* **2021**, *11*, 8950. [CrossRef] [PubMed]
26. Segundo, F.A.d.S.; Costa, E.I.d.S.; Azevedo, A.S.d.; Araújo, A.L.d.; Silva, A.C.d.F.; de Lima, G.G.; de Sá, M.J.C. Platelet-rich plasma, hydroxyapatite, and chitosan in the bone and cartilaginous regeneration of femoral trochlea in rabbits: Clinical, radiographic, and histomorphometric evaluations. *J. Healthc. Eng.* **2018**, *2018*, 6917958. [CrossRef] [PubMed]
27. Shah, S.R.; Young, S.; Goldman, J.L.; Jansen, J.A.; Wong, M.E.; Mikos, A.G. A composite critical-size rabbit mandibular defect for evaluation of craniofacial tissue regeneration. *Nat. Protoc.* **2016**, *11*, 1989–2009. [CrossRef] [PubMed]
28. Aguilar, A.; Zein, N.; Harmouch, E.; Hafdi, B.; Bornert, F.; Offner, D.; Clauss, F.; Fioretti, F.; Huck, O.; Benkirane-Jessel, N. Application of chitosan in bone and dental engineering. *Molecules* **2019**, *24*, 3009. [CrossRef] [PubMed]
29. Al-Fotawei, R.; Ayoub, A.F.; Heath, N.; Naudi, K.B.; Tanner, K.E.; Dalby, M.J.; McMahon, J. Radiological assessment of bioengineered bone in a muscle flap for the reconstruction of critical-size mandibular defect. *PLoS ONE* **2014**, *9*, e107403. [CrossRef] [PubMed]
30. Suvarna, K.S.; Layton, C.; Bancroft, J.D. *Bancroft's Theory and Practice of Histological Techniques E-Book*; Elsevier Health Sciences: Amsterdam, The Netherlands, 2018.
31. Gholipour, H.; Meimandi-Parizi, A.; Oryan, A.; Bigham Sadegh, A. The effects of gelatin, fibrin-platelet glue and their combination on healing of the experimental critical bone defect in a rat model: Radiological, histological, scanning ultrastructural and biomechanical evaluation. *Cell Tissue Bank.* **2018**, *19*, 341–356. [CrossRef]
32. Abdo, W.; Ghattas, S.; Sakai, H.; Hirata, A.; Yanai, T. Assessment of proliferative activity by proliferative cell nuclear antigen (PCNA) and anti-bromodeoxyuridine (BrdU) immunolabeling in the tissues of japanese eels (*Anguilla japonica*). *Turk. J. Fish. Aquat. Sci.* **2014**, *14*, 413–419. [CrossRef]
33. Chang, S.-H.; Hsu, Y.-M.; Wang, Y.J.; Tsao, Y.-P.; Tung, K.-Y.; Wang, T.-Y. Fabrication of pre-determined shape of bone segment with collagen-hydroxyapatite scaffold and autogenous platelet-rich plasma. *J. Mater. Sci. Mater. Med.* **2009**, *20*, 23–31. [CrossRef]
34. Lim, J.; Donahue, H.J. Biomaterial characteristics important to skeletal tissue engineering. *J. Musculoskelet. Neuronal Interact.* **2004**, *4*, 396. [PubMed]
35. Thomaidis, V.; Kazakos, K.; Lyras, D.N.; Dimitrakopoulos, I.; Lazaridis, N.; Karakasis, D.; Botaitis, S.; Agrogiannis, G. Comparative study of 5 different membranes for guided bone regeneration of rabbit mandibular defects beyond critical size. *Med. Sci. Monit.* **2008**, *14*, BR67–BR73. [PubMed]
36. Schmitz, J.P.; Hollinger, J.O. The critical size defect as an experimental model for craniomandibulofacial nonunions. *Clin. Orthop. Relat. Res.* **1986**, *205*, 299–308. [CrossRef]
37. Oryan, A.; Sahvieh, S. Effectiveness of chitosan scaffold in skin, bone and cartilage healing. *Int. J. Biol. Macromol.* **2017**, *104*, 1003–1011. [CrossRef]
38. Cheng, G.; Li, Z.; Wan, Q.; Lv, K.; Li, D.; Xing, X.; Li, Z. A novel animal model treated with tooth extraction to repair the full-thickness defects in the mandible of rabbits. *J. Surg. Res.* **2015**, *194*, 706–716. [CrossRef]
39. Sivashankari, P.; Prabaharan, M. Prospects of chitosan-based scaffolds for growth factor release in tissue engineering. *Int. J. Biol. Macromol.* **2016**, *93*, 1382–1389. [CrossRef]
40. Nair, P.N.R. On the causes of persistent apical periodontitis: A review. *Int. Endod. J.* **2006**, *39*, 249–281. [CrossRef]
41. Amine, K.; Gharibi, A.; Hsaine, A.; Kissa, J. Effect of bone regeneration with mineralized plasmatic matrix for implant placement in aesthetic zone. *Case Rep. Dent.* **2017**, *2017*, 2639564. [CrossRef]

42. Moheb, M.E.; Al-Zarea, B.; Sghaireen, M.G.; Toriya, J.; Mizohata, A.; Patil, S.; Siada, A.; Brad, B.; Kochaji, N.; Alam, M.K. Mineralized plasmatic matrix to enhance the bone grafting technique. *J. Hard Tissue Biol.* **2017**, *26*, 289–292. [CrossRef]
43. Lawrence, T. The nuclear factor NF-κB pathway in inflammation. *Cold Spring Harb. Perspect. Biol.* **2009**, *1*, a001651. [CrossRef]
44. Wang, Y.; Ni, H.; Li, H.; Deng, H.; Xu, L.S.; Xu, S.; Zhen, Y.; Shen, H.; Pan, H.; Yao, M. Nuclear factor kappa B regulated monocyte chemoattractant protein-1/chemokine CC motif receptor-2 expressing in spinal cord contributes to the maintenance of cancer-induced bone pain in rats. *Mol. Pain* **2018**, *14*, 1744806918788681. [CrossRef] [PubMed]
45. Takayanagi, H. Inflammatory bone destruction and osteoimmunology. *J. Periodontal Res.* **2005**, *40*, 287–293. [CrossRef] [PubMed]
46. Elsharkawy, A.M.; Mann, D.A. Nuclear factor-κB and the hepatic inflammation-fibrosis-cancer axis. *Hepatology* **2007**, *46*, 590–597. [CrossRef] [PubMed]
47. Lee, S.-K.; Lorenzo, J. Cytokines regulating osteoclast formation and function. *Curr. Opin. Rheumatol.* **2006**, *18*, 411–418. [CrossRef] [PubMed]
48. Khosla, S. Minireview: The opg/rankl/rank system. *Endocrinology* **2001**, *142*, 5050–5055. [CrossRef]
49. Hong, S.; Hsu, H.-J.; Kaunas, R.; Kameoka, J. Collagen microsphere production on a chip. *Lab Chip* **2012**, *12*, 3277–3280. [CrossRef]
50. Arai, Y.; Choi, B.; Kim, B.J.; Park, S.; Park, H.; Moon, J.J.; Lee, S.-H. Cryptic ligand on collagen matrix unveiled by MMP13 accelerates bone tissue regeneration via MMP13/Integrin α3/RUNX2 feedback loop. *Acta Biomater.* **2021**, *125*, 219–230. [CrossRef]
51. Intini, G. The use of platelet-rich plasma in bone reconstruction therapy. *Biomaterials* **2009**, *30*, 4956–4966. [CrossRef]
52. Rahman, S.; Sutedja, E.; Ayu, O.; Amirsyah, M. The Effect of Platelet-Rich Plasma on Type I Collagen Production, VEGF Expression, and Neovascularization after Femoral Bone Implants: A Study on Rat Models. *Orthop. Res. Rev.* **2022**, *14*, 207. [CrossRef]
53. Kim, Y.-K.; Kim, S.-G.; Oh, J.-S.; Jin, S.-C.; Son, J.-S.; Kim, S.-Y.; Lim, S.-Y. Analysis of the inorganic component of autogenous tooth bone graft material. *J. Nanosci. Nanotechnol.* **2011**, *11*, 7442–7445. [CrossRef]
54. Gomes, M.F.; Da Silva Dos Anjos, M.J.; de Oliveira Nogueira, T.; Guimarães, S.A.C. Histologic evaluation of the osteoinductive property of autogenous demineralized dentin matrix on surgical bone defects in rabbit skulls using human amniotic membrane for guided bone regeneration. *Int. J. Oral Maxillofac. Implant.* **2001**, *16*, 563–571.
55. Rocha, C.A.; Cestari, T.M.; Vidotti, H.A.; de Assis, G.F.; Garlet, G.P.; Taga, R. Sintered anorganic bone graft increases autocrine expression of VEGF, MMP-2 and MMP-9 during repair of critical-size bone defects. *J. Mol. Histol.* **2014**, *45*, 447–461. [CrossRef] [PubMed]
56. Schipani, E.; Maes, C.; Carmeliet, G.; Semenza, G.L. Regulation of osteogenesis-angiogenesis coupling by HIFs and VEGF. *J. Bone Miner. Res.* **2009**, *24*, 1347–1353. [CrossRef] [PubMed]
57. Taylor, C.T. Interdependent roles for hypoxia inducible factor and nuclear factor-κB in hypoxic inflammation. *J. Physiol.* **2008**, *586*, 4055–4059. [CrossRef]
58. Page-McCaw, A.; Ewald, A.J.; Werb, Z. Matrix metalloproteinases and the regulation of tissue remodelling. *Nat. Rev. Mol. Cell Biol.* **2007**, *8*, 221–233. [CrossRef] [PubMed]
59. Ortega, N.; Behonick, D.; Stickens, D.; Werb, Z. How proteases regulate bone morphogenesis. *Ann. N. Y. Acad. Sci.* **2003**, *995*, 109–116. [CrossRef]
60. Davis, G.E.; Senger, D.R. Endothelial extracellular matrix: Biosynthesis, remodeling, and functions during vascular morphogenesis and neovessel stabilization. *Circ. Res.* **2005**, *97*, 1093–1107. [CrossRef]
61. Ortega, N.; Behonick, D.J.; Werb, Z. Matrix remodeling during endochondral ossification. *Trends Cell Biol.* **2004**, *14*, 86–93. [CrossRef]
62. Karsdal, M.A.; Larsen, L.; Engsig, M.T.; Lou, H.; Ferreras, M.; Lochter, A.; Delaissé, J.-M.; Foged, N.T. Matrix metalloproteinase-dependent activation of latent transforming growth factor-β controls the conversion of osteoblasts into osteocytes by blocking osteoblast apoptosis. *J. Biol. Chem.* **2002**, *277*, 44061–44067. [CrossRef]
63. Zwingenberger, B.; Vater, C.; Bell, R.L.; Bolte, J.; Mehnert, E.; Brünler, R.; Aibibu, D.; Zwingenberger, S. Treatment of Critical-Size Femoral Bone Defects with Chitosan Scaffolds Produced by a Novel Process from Textile Engineering. *Biomedicines* **2021**, *9*, 1015. [CrossRef]
64. Rodríguez-Merchán, E.C. Bone healing materials in the treatment of recalcitrant nonunions and bone defects. *Int. J. Mol. Sci.* **2022**, *23*, 3352. [CrossRef] [PubMed]
65. Peng, H.; Usas, A.; Olshanski, A.; Ho, A.M.; Gearhart, B.; Cooper, G.M.; Huard, J. VEGF improves, whereas sFlt1 inhibits, BMP2-induced bone formation and bone healing through modulation of angiogenesis. *J. Bone Miner. Res.* **2005**, *20*, 2017–2027. [CrossRef] [PubMed]
66. Wernike, E.; Montjovent, M.-O.; Liu, Y.; Wismeijer, D.; Hunziker, E.B.; Siebenrock, K.-A.; Hofstetter, W.; Klenke, F.M. VEGF incorporated into calcium phosphate ceramics promotes vascularisation and bone formation in vivo. *Eur. Cell Mater.* **2010**, *19*, 30–40. [PubMed]